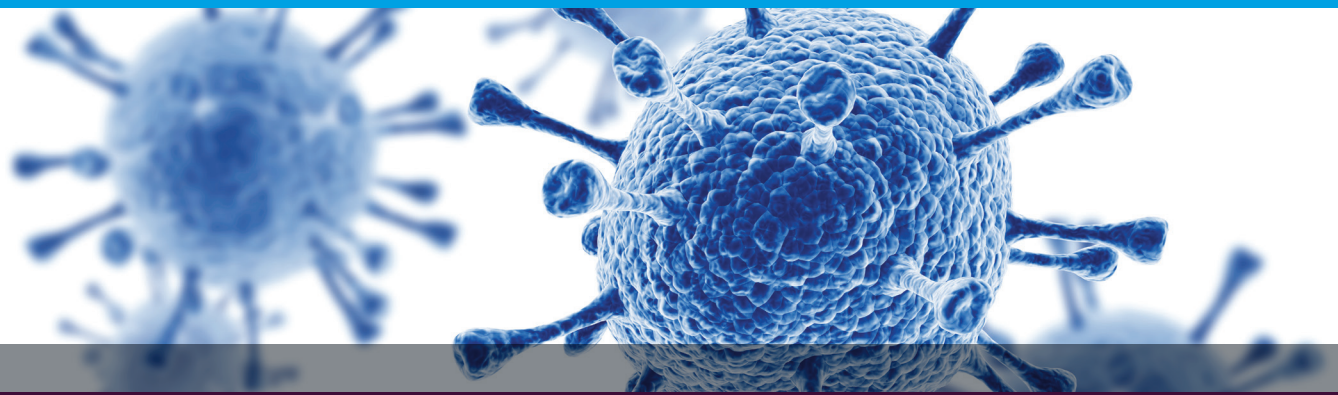


# Vaccine and Virology Applications

Agilent xCELLigence RTCA handbook



# Table of Contents

<b>Overview</b>	<b>4</b>
Importance of the cytopathic effect in virology research	4
Shortcomings of traditional CPE assays	4
The solution: xCELLigence real-time CPE assay	5
E-Plates	7
Real-time impedance traces explained	7
xCELLigence instruments	8
<b>Applications</b>	<b>9</b>
Virus titer determination	9
Detection and quantification of neutralizing antibodies	11
Studying antiviral drugs	13
Testing virucides	16
Oncolytic viruses	17
Characterizing virus quality/fitness	19

# Overview

## Importance of the cytopathic effect in virology research

When infected with a virus, host cells often display microscopically visible changes that are collectively referred to as a cytopathic effect (CPE). CPEs can include cell shrinkage or enlargement, deterioration/lysis, cell fusion, and the formation of inclusion bodies. Not all viruses cause a CPE in their host cell, but if they do, it can be a useful tool for various research applications, including everything from virus titer determination to the detection and quantification of neutralizing antibodies.

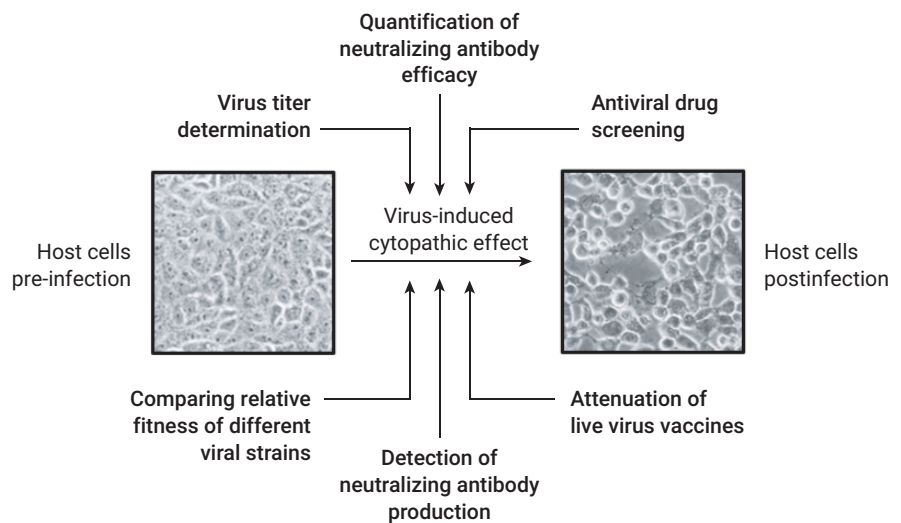


Figure 1. Factors contributing to cytopathic effect.

## Shortcomings of traditional CPE assays

In a typical CPE assay, a monolayer of cells is infected with a virus and then monitored over several days (or weeks) to track morphological changes. These changes emerge in distinct foci corresponding to sites of infection. For many decades, the assay of choice has been the plaque assay, where shortly after being infected, the monolayer of cells is overlaid with a semisolid material such as agarose. As infected cells lyse, the agarose prevents progeny virions from freely diffusing through the medium and infecting cells at distant locations in the well. Only neighboring cells are infected because the virus can only diffuse laterally beneath the agarose layer. As this cycle of infection, lysis, and infection of adjacent cells continues, a cell-free region known as a plaque forms, which can be counted by eye or under a microscope. There are numerous variations of the plaque assay (with or without staining cells, for example), but all are labor intensive. Determining what is or is not a legitimate plaque is difficult. This makes achieving high levels of accuracy and reproducibility challenging. Finally, kinetic information is difficult to derive from the endpoint data of a plaque assay. This kinetic information may be useful when comparing the relative fitness of two different virus strains/isolates.

The use of a virus that has been engineered to express a fluorescent protein can make it easier to identify sites of infection within the monolayer of host cells. But in many contexts (such as the development of a live attenuated viral vaccine), this type of modification to the viral genome is not permissible. As an alternative, identifying infected cells using antibodies against virus proteins coupled with fluorescence microscopy can be useful but requires substantial hands-on time and reagents can be expensive. Another problem with the above two types of fluorescence-based assays is that they do not provide an assessment/quantification of the full virus life cycle. For example, a viral strain may be capable of infecting cells and expressing fluorescent protein, but still display deficiencies in downstream steps such as capsid assembly or lysis of the host cell. In this context, tracking the presence of viral protein by fluorescence is not appropriate for evaluating virus fitness/quality.

The solution: Agilent  
xCELLigence real-time  
CPE assay

As a more efficient and higher-throughput alternative to traditional CPE assays, a large number of labs in industrial and academic settings are now using Agilent xCELLigence real-time cell analysis (RTCA) instruments for many virology applications.



**Figure 2.** Example of an Agilent xCELLigence instrument. xCELLigence instruments are available in different formats (16-, 48-, 96-, and 576-wells). The instrument shown contains six cradles, each of which houses an electronic 96-well microplate. The plate-housing portion of the instrument is placed inside a standard tissue culture incubator, while the analyzer and control unit (a laptop computer) are housed outside the incubator. All six plates can be monitored simultaneously and independently of one another, maximizing throughput and flexibility.

xCELLigence instruments use patented microplates (Agilent E-Plates) that contain gold biosensors integrated into the bottom of each well. When submerged in an electrically conductive solution (such as a standard tissue culture medium), the application of a weak electric potential across these biosensors causes a miniscule electric current to flow between them (Figure 3B). The presence of adherent cells on the gold biosensors impedes current flow and the magnitude of this impedance depends on the number of cells, the size of the cells, the cell-substrate attachment quality, and cell-cell adhesion (barrier function). Neither the gold biosensor surfaces nor the electric potential has an effect on cell health or behavior.

In the context of virology assays, infected cells that progress through the continuum of the cytopathic effect (displaying rounding and eventually detachment or lysis) become increasingly less effective at impeding the flow of electric current (Figure 3B). xCELLigence detects subtle changes that go undetected by microscopy, such as reduced cell-surface adhesion strength. By measuring these changes continuously, xCELLigence tracks viral CPEs in unprecedented detail and yields quantitative kinetics that can be used for numerous applications.

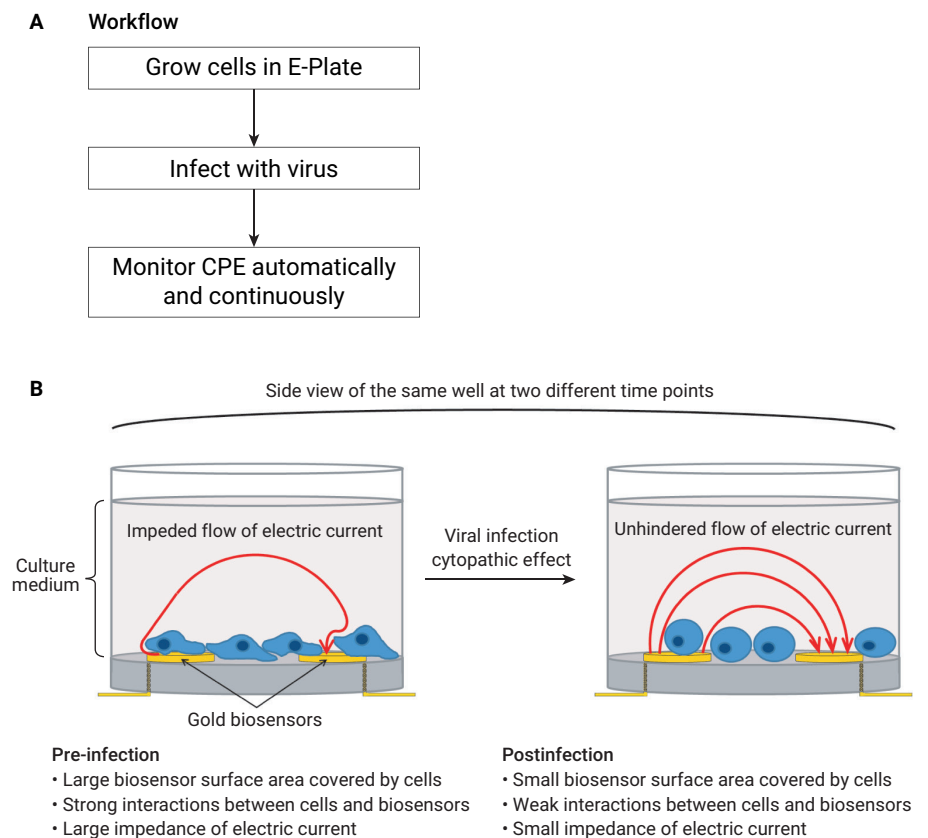


**Figure 3.** Using an Agilent xCELLigence instrument to monitor viral CPE in real time. (A) Simple workflow to monitor viral CPE. Once cells have been infected, no further hands-on time is required; data acquisition is automated and continuous. (B) Gold biosensors monitor real-time virus-induced changes in cell number, size, cell-substrate attachment quality, and cell-cell adhesion.

## E-Plates

In contrast to the simplified example in Figure 3, the gold biosensors in Agilent E-Plates are arranged as an interdigitated array that covers approximately 75% of each well bottom surface area. This enables thousands of cells to be analyzed en masse, which provides exquisite sensitivity to real-time changes in cell health and behavior.

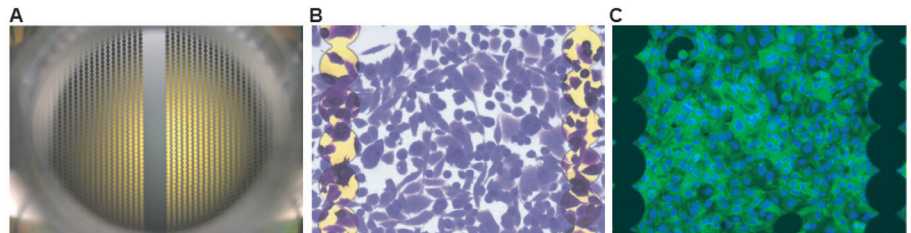


**Figure 4.** Impedance biosensors on Agilent E-Plates. (A) Photograph of a single well in an E-Plate. Though cells can be visualized on the gold biosensor surfaces, the electrode-free region in the middle of the well facilitates microscopic imaging. (B) Zoomed in view of the gold biosensors and crystal violet-stained human cells, as seen by epi-illumination microscopy. (C) Immunofluorescence microscopy with gold biosensors silhouetted.

## Real-time impedance traces explained

The impedance of electric current caused by adherent cells is reported using a unitless parameter called Cell Index (CI), where:

$$CI = \frac{(\text{Impedance at time point } n) - (\text{Impedance with no cells})}{(\text{nominal impedance constant})}$$


Figure 5 provides a generic example of a real-time impedance trace throughout the course of setting up and running a viral CPE assay. For the first few hours after cells have been added to a well, there is a rapid increase in impedance caused by cell attachment and spreading. If cells are subconfluent after the initial attachment stage, they will start to proliferate and cause a gradual yet steady increase in CI. When cells reach confluence, the CI value plateaus because the entire surface area of the biosensor has become saturated. Infection with a CPE-inducing virus subsequently causes a steady decrease in CI. A drop in CI back to zero reflects the total lysis or detachment of the target cells. This correlation between the impedance signal and the presence/status of cells on the biosensors is easily confirmed through microscopy.

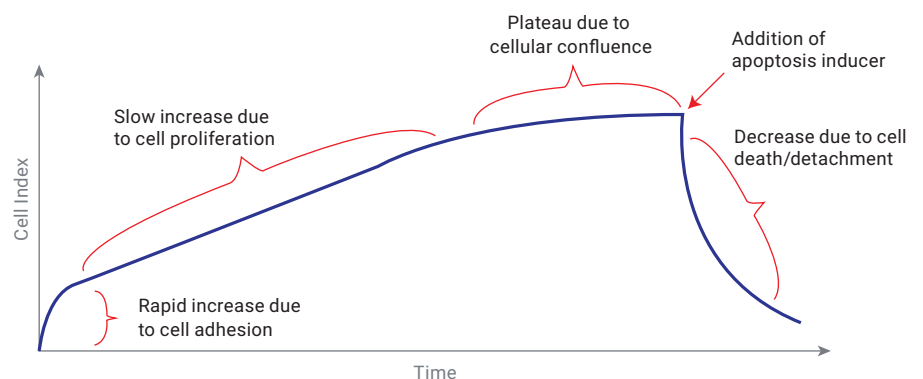


**Figure 5.** Generic real-time impedance trace for setting up and running a viral CPE assay. Each phase of the impedance trace and the cellular behavior is explained in the text.

## xCELLigence instruments

The nine different xCELLigence instruments all employ noninvasive electrical impedance monitoring to track cell health and behavior, as described on the preceding two pages. The table below shows the four xCELLigence instruments best suited for vaccine development and general virology studies. In addition to differing in their plate format/throughput, some of the instruments possess specialized functionalities, such as the ability to monitor cell invasion and migration.



	Dual Purpose (DP)	Single Plate (SP)	Multiple Plates (MP)	High Throughput (HT)	eSight
Format	3 × 16 wells	1 × 96 wells	6 × 96 wells	1 × 384 wells	3 × 96 wells impedance, 5 × 96 wells imaging
Maximum throughput	48 wells	96 wells	576 wells	Up to 4 × 382 wells (1,536 wells total)	288 wells impedance, up to 480 wells total for imaging



**Figure 6.** Live cell analysis directly inside an incubator. Placed inside a standard tissue culture incubator or hypoxia chamber, Agilent xCELLigence instruments are compatible with the full range of biologically relevant temperatures, atmospheric compositions, and humidities.

# Applications

## Virus titer determination

Since the traditional CPE/plaque assays used for quantifying viral titers are labor-intensive and time-consuming, Reisen and colleagues evaluated the efficacy of xCELLigence RTCA for determining the titers of West Nile virus (WNV) and St. Louis encephalitis virus (SLEV).<sup>1</sup> Vero cells in suspension were incubated with serial dilutions of a known concentration of WNV or SLEV for 30 minutes at 37 °C. This was followed by immediate addition of the cell/virus suspension to E-Plate wells and subsequent monitoring of impedance in an xCELLigence instrument. In contrast to uninfected control cells, which grew to confluency and maintained a plateaued CI, virus-infected cells displayed a time-dependent decrease in CI to zero, indicating complete cell lysis (upper panels of Figures 7A and 7B). Consistent with the known cytolytic activities of WNV and SLEV, xCELLigence displays WNV to have an earlier onset of CPE and a more rapid rate of CPE progression.

For WNV and SLEV, the time at which the cytopathic effect occurred correlated with the known titer of the virus. This was highlighted by plotting the CIT50 (time required for the CI to decrease by 50%) as a function of virus titer (lower panels of Figures 7A and 7B). Using this type of standard curve, determining the viral titer in samples of unknown concentration was possible. Beyond characterizing viral stocks used for research or vaccine purposes, this approach can be applied in the lab to quantify the load of a specific virus before, during, and after exposure.



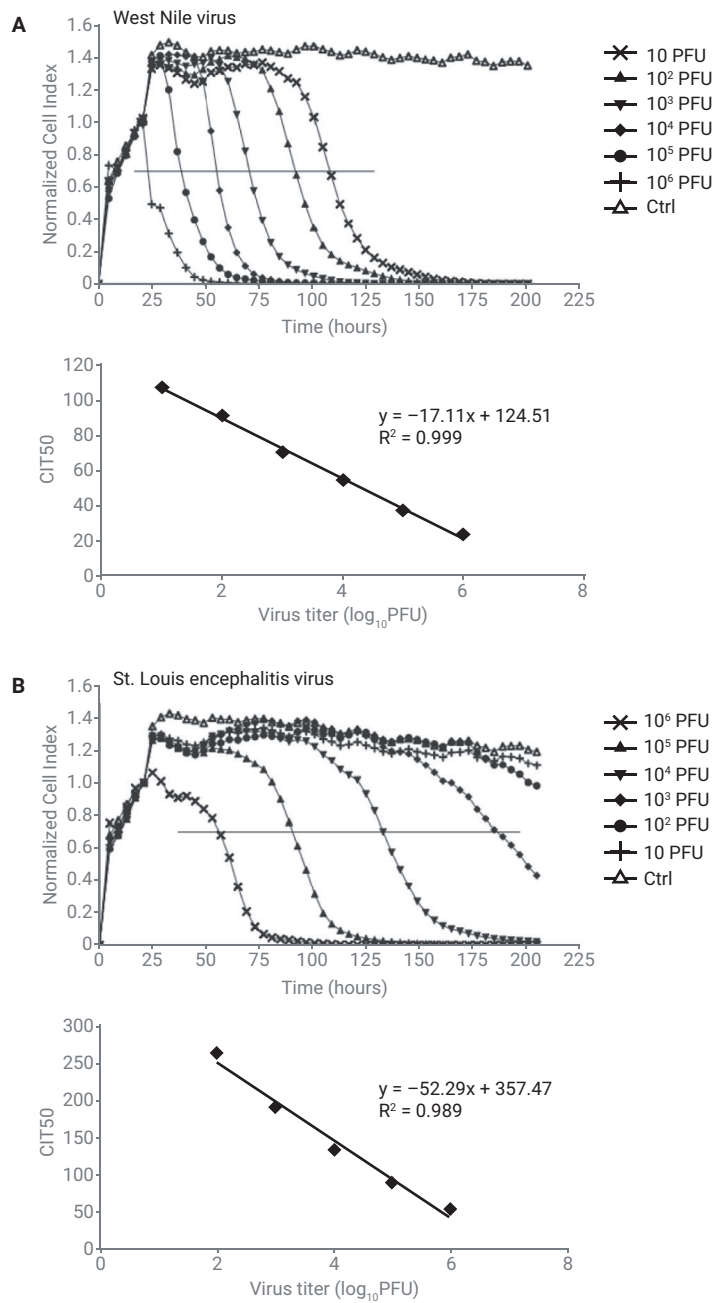


**Figure 7.** Using Agilent xCELLigence RTCA to determine viral titer. (A) Upper panel: real-time monitoring of WNV-induced cytopathic effect in Vero cells. The normalized Cell Index is shown for E-Plate wells that were inoculated with a negative control (Ctrl) or different numbers of plaque forming units (PFUs) of WNV. Each curve is an average of two independent replicate wells. The horizontal line denotes the point at which CI has dropped to 50% of its initial value (before virus addition). The time required to reach this point is referred to as CIT50. Lower panel: by plotting CIT50 as a function of viral titer, a standard curve was produced, which can be used for determining virus concentration in diverse types of samples. (B) Real-time monitoring of SLEV-induced cytopathic effect in Vero cells. Experimental details and data processing are similar to part (A).

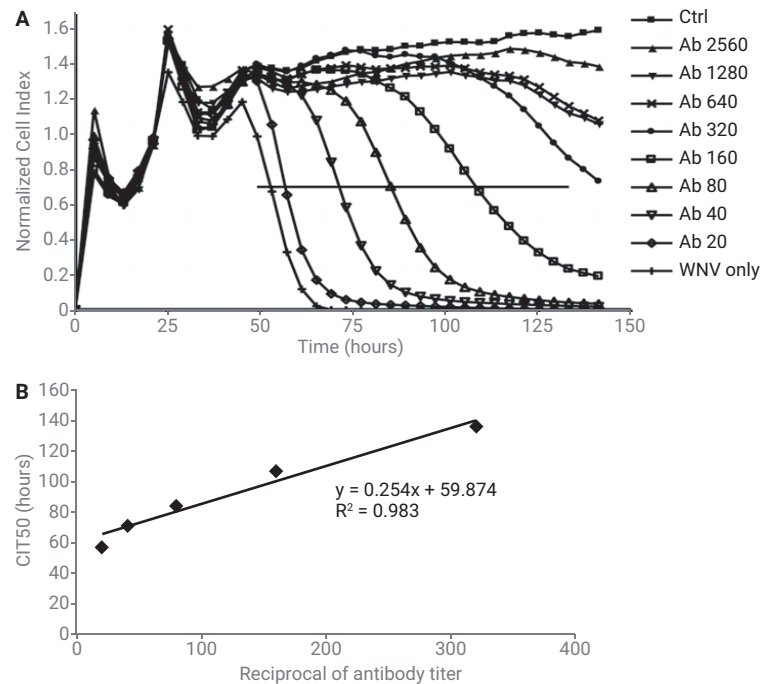
Figure reprinted from *Journal of Virological Methods*, volume 173(2), Fang, Y. *et al.*, "Real-Time Monitoring of Flavivirus Induced Cytopathogenesis Using Cell Electric Impedance Technology," pages 251–8. Copyright 2011, with permission from Elsevier.

References—using  
xCELLigence for virus titer  
determination

1. Fang, Y. *et al.* Real-Time Monitoring of Flavivirus Induced Cytopathogenesis Using Cell Electric Impedance Technology. *J. Virol. Methods* **2011** May, *173*(2), 251–8.
2. Witkowski, P. T. *et al.* Cellular Impedance Measurement as a New Tool for Poxvirus Titration, Antibody Neutralization Testing and Evaluation of Antiviral Substances. *Biochem. Biophys. Res. Commun.* **2010** Oct 8, *401*(1), 37–41.
3. Charretier, C. *et al.* Robust Real-Time Cell Analysis Method for Determining Viral Infectious Titers During Development of a Viral Vaccine Production Process. *J. Virol. Methods* **2017** Nov 14, *252*, 57–64.

## Detection and quantification of neutralizing antibodies

The xCELLigence function for tracking virus-induced CPEs in real time can be used for detecting and quantifying neutralizing antibodies. The assay principle is similar to a standard plaque reduction neutralization test, but the automated data acquisition of the xCELLigence instrument dramatically reduces the hands-on time required and eliminates subjectivity in the data analysis. The two examples shown in Figure 8 demonstrate the usefulness of this approach for research applications.



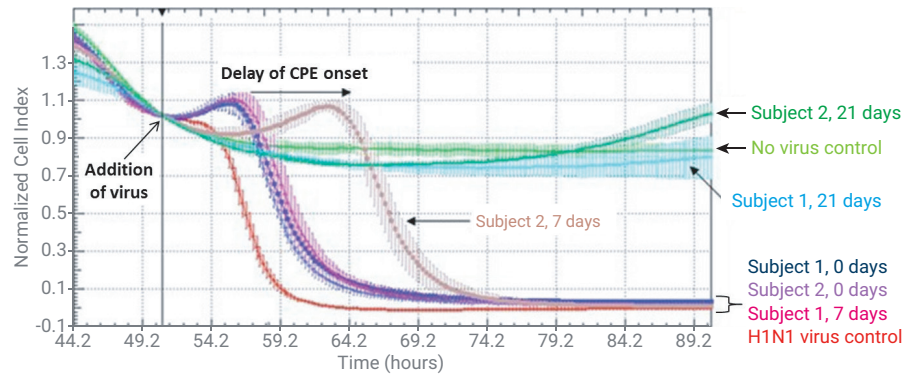
**Figure 8.** Quantifying WNV neutralizing antibody titer using Agilent xCELLigence RTCA. (A) Vero cells were infected with  $10^6$  PFU of WNV that were pre-incubated with different dilutions of neutralizing antibody. Ctrl = Vero cells that were not infected with virus; WNV only = Vero cells infected with virus that was not pre-exposed to antibody. The horizontal line denotes the point at which Cell Index has dropped to 50% of its initial value (that is, before virus addition). The time required to reach this point is referred to as CIT50. (B) By plotting CIT50 as a function of the reciprocal of antibody titer, a standard curve is produced which can be used for assessing the antibody concentration in wild avian sera.

Figure reprinted from *Journal of Virological Methods*, volume 173(2), Fang, Y. et al., "Real-Time Monitoring of Flavivirus Induced Cytopathogenesis Using Cell Electric Impedance Technology," pages 251–8. Copyright 2011, with permission from Elsevier.

After growing Vero cells to confluence in E-Plate wells, Fang and coworkers infected each well with  $10^6$  plaque forming units (PFU) of WNV that had been pre-incubated with serially diluted neutralizing antibody of known concentration.<sup>1</sup> As shown in Figure 8A, the onset of WNV-induced CPE was delayed by the neutralizing antibody in a manner that was directly dependent on antibody concentration. By plotting the CIT50 (time required for the CI to decrease by 50%) as a function of the reciprocal of the antibody titer, a standard curve was generated (Figure 8B). This could be used for quantifying the amount of neutralizing antibody present in avian specimens. Using this xCELLigence-based standard curve to determine antibody concentrations in infected birds in the wild gave values that correlated with values determined by a traditional plaque reduction neutralization test.<sup>1</sup>

Similarly to the WNV method, xCELLigence has been used for quantifying the amount of neutralizing antibody against influenza A H1N1 virus that is present in human sera (Figure 9). Confluent cells in E-Plate wells were infected with purified H1N1 virus that either had or had not been pretreated with subject's serum. These serum samples were collected before vaccination, and 7 or 21 days postvaccination, to track the emergence of the H1N1-specific neutralizing response over time. As expected, the robustness of the H1N1 neutralizing antibody activity increased progressively over the first 21 days postvaccination, evidenced by the delayed onset or complete block of the cytopathic effect.

With its simple, automated workflow and objective and quantitative readout, xCELLigence clearly offers advantages over traditional assays for detecting and quantifying neutralizing antibodies. This approach provides a simple means for monitoring the efficacy of vaccination, and for elucidating the kinetics of virus resistance emergence.



**Figure 9.** Measuring neutralizing antibody activity in H1N1-vaccinated subjects using Agilent xCELLigence. Serum samples from two subjects were collected before vaccination (day 0), then 7 and 21 days postvaccination. These serum samples were incubated with purified H1N1 virus before adding the virus/serum mixture to cells growing in an Agilent E-Plate. For both subjects, serum from day 0 (purple and blue curves) provides no protection, and the virus kills the cells with kinetics similar to the positive control (red curve). For subject 2, serum from day 7 showed significant delay of H1N1-induced CPE (brown curve), indicating the presence of specific neutralizing antibodies against H1N1 virus. Conversely, subject 1's serum at day 7 showed no prophylactic effect (pink curve), indicating that an H1N1 neutralizing antibody activity was not yet present. However, 21 days postvaccination the serum from both subjects displayed robust neutralizing antibody activity against H1N1, rendering the virus completely incapable of inducing a cytopathic effect (dark green and aqua curves). This assay makes it possible to quantitatively assess the efficacy of a particular vaccine, as well as the kinetics of virus resistance emergence.

Figure adapted from *Asia Pacific Biotech News*, volume 14(10), Lu, H. *et al.* "Label-free Real-time Cell Based Assay System for Evaluating H1N1 Vaccination Success," pages 31–32. Copyright 2010, with permission from Asia Pacific Biotech News.

References—using  
xCELLigence to detect  
and quantify neutralizing  
antibodies

1. Fang, Y. *et al.* Real-time Monitoring of Flavivirus Induced Cytopathogenesis Using Cell Electric Impedance Technology. *J. Virol. Methods* **2011** May, *173*(2), 251–8.
2. Label-free Real-time Cell Based Assay System for Evaluating H1N1 Vaccination Success. *Asia Pacific Biotech News* **2010**, *14*(10), 31–32.
3. Teng, Z. *et al.* Real-Time Cell Analysis—a New Method for Dynamic, Quantitative Measurement of Infectious Viruses and Antiserum Neutralizing Activity. *J. Virol. Methods* **2013** Nov, *193*(2), 364–70.
4. Kashima, K. *et al.* Inhibition of Metastasis of Rhabdomyosarcoma by a Novel Neutralizing Antibody to CXCR4 Chemokine Receptor-4. *Cancer Sci.* **2014** Oct, *105*(10), 1343–50.
5. Tian, D. *et al.* Novel, Real-Time Cell Analysis for Measuring Viral Cytopathogenesis and the Efficacy of Neutralizing Antibodies to the 2009 Influenza A (H1N1) Virus. *PLoS One* **2012**, *7*(2), e31965.

## Studying antiviral drugs

xCELLigence is an excellent tool for identifying and characterizing drugs that inhibit any facet of the virus lifecycle because real-time impedance monitoring is sensitive to virus-induced cytopathic effects. In one example, Urs Greber and colleagues aimed to identify a drug that could mitigate the effects of adenovirus in subjects already infected with the virus. Their screening assay involved growing HeLa cells to confluence, then infecting them with human adenovirus in the presence of different drug candidates. Most effective among these was flavopiridol, a semisynthetic flavonoid compound known to inhibit the cell cycle-dependent kinase Cdk9. As shown in Figure 10A, in the absence of drugs, the adenovirus infection induced a robust CPE, evidenced by the impedance signal decreasing to zero (red curve). However, in a dose-dependent manner, flavopiridol was able to significantly delay the onset of CPE (blue and orange curves). These impedance-based findings were corroborated by microscopy analysis (Figure 10B).

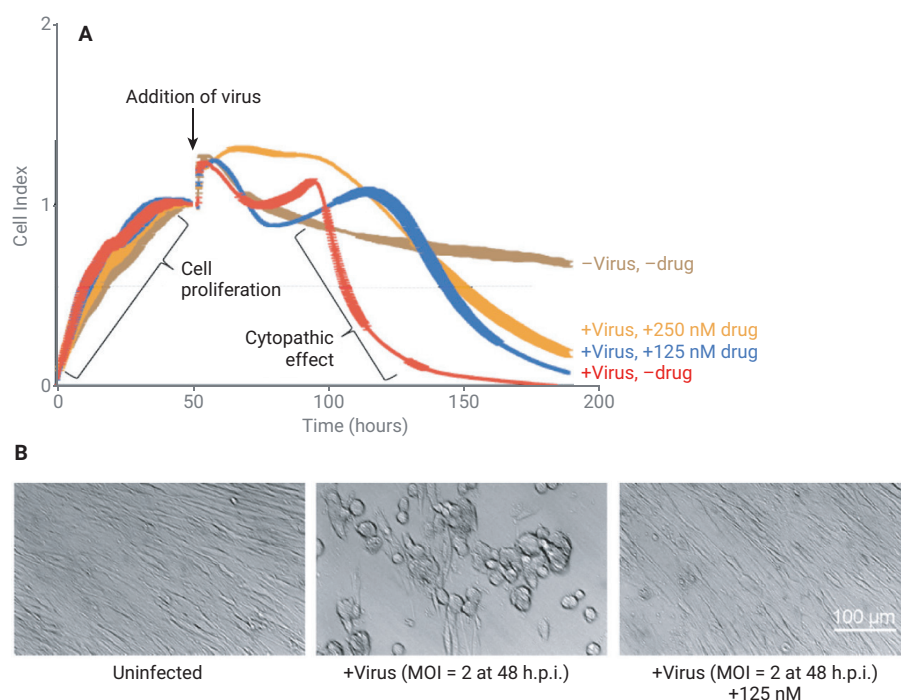


**Figure 10.** Monitoring antiviral activity of flavopiridol. (A) HeLa cells were grown in an Agilent E-Plate to the point of confluence. Roughly 50 hours postseeding, cells were infected with human adenovirus strain C5 in the presence of different concentrations of flavopiridol. (B) Flavopiridol affords broad protection against adenovirus. Here, WI38 lung fibroblasts were infected with human adenovirus strain D37, and four hours later, flavopiridol either was or was not added. 48 hours postinfection, the drug is clearly seen to have prevented a cytopathic effect from occurring.

Figure adapted with permission from *ACS Infectious Diseases*, volume 3(6), Prasad, V. *et al.* "Cell Cycle-Dependent Kinase Cdk9 Is a Postexposure Drug Target Against Human Adenoviruses," pages 398–405. Copyright 2017, American Chemical Society.

In a second example, Guy Boivin and coworkers analyzed the sensitivity of wildtype (WT) and mutant herpes simplex virus 1 (HSV-1) to the antiviral acyclovir. After being grown to confluence in E-Plates, Vero cells were infected with the virus for 90 minutes before adding different concentrations of the drug. The CPE induced by both WT and mutant virus could be blocked by acyclovir, but a much higher concentration of the drug was required for blocking the mutant strain than the WT strain (Figure 11).

By plotting the CI value at a given time point as a function of drug concentration, dose response curves were generated (data not shown here), yielding EC<sub>50</sub> values of 100 μm and 0.8 μm for the mutant and WT viruses, respectively. These findings were consistent with this particular mutant strain of the virus having a mutation in its DNA polymerase, which is the target of acyclovir.

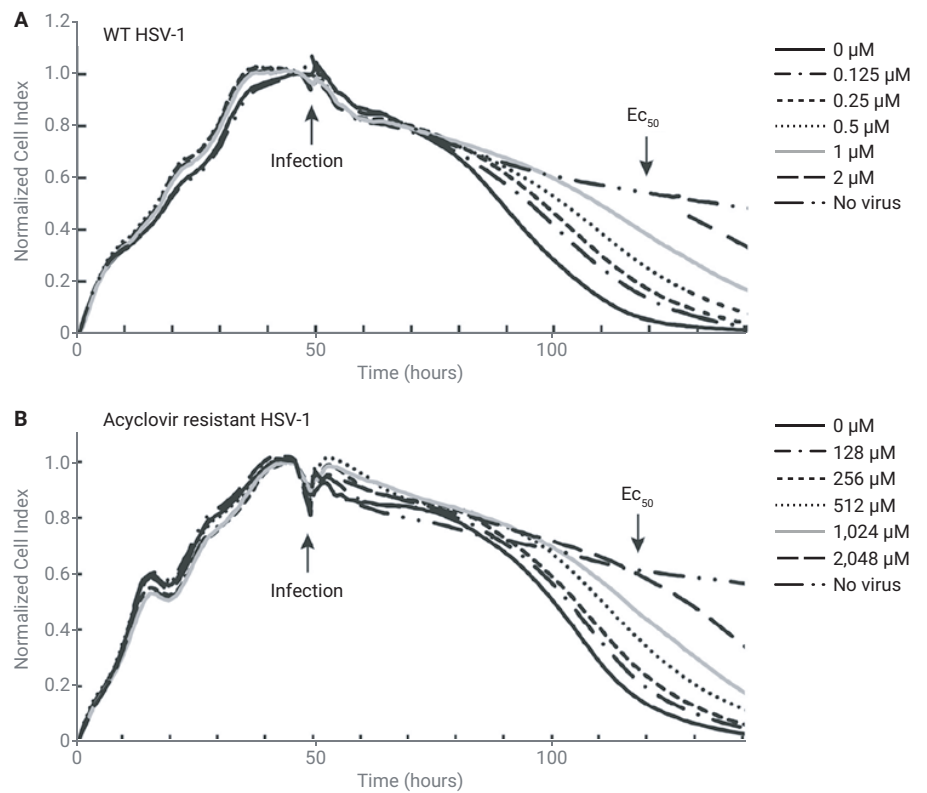


**Figure 11.** Comparing acyclovir sensitivity of WT and mutant HSV-1. Vero cells were grown to confluence in an Agilent E-Plate. 48 hours postseeding, cells were infected with either WT or mutant HSV-1 for 90 minutes. Different concentrations of acyclovir were then added, and impedance was monitored every 30 minutes for an additional 100 hours. Note that much higher concentrations of the drug were required to prevent the cytopathic effect in the mutant.

Data adapted from the *Journal of Clinical Microbiology*, volume 54(8), Piret, J. et al. "Novel Method Based on Real-Time Cell Analysis for Drug Susceptibility Testing of Herpes Simplex Virus and Human Cytomegalovirus." Copyright 2016, with permission from American Society for Microbiology.

## References—using xCELLigence for viral drug screening

1. Watterson, D. *et al.* A Generic Screening Platform For Inhibitors of Virus Induced Cell Fusion Using Cellular Electrical Impedance. *Sci. Rep.* **2016** Mar 15, 6, 22791.
2. Zandi, K. A Real-Time Cell Analyzing Assay for Identification of Novel Antiviral Compounds against Chikungunya Virus. *Methods Mol. Biol.* **2016**, 1426, 255–62.
3. Sharma, B. N. *et al.* Antiviral Effects of Artesunate on Polyomavirus BK Replication in Primary Human Kidney Cell. *Antimicrob. Agents Chemother.* **2014**, 58(1), 279–89.
4. Witkowski, P. T. *et al.* Cellular Impedance Measurement as a New Tool for Poxvirus Titration, Antibody Neutralization Testing and Evaluation of Antiviral Substances. *Biochem. Biophys. Res. Commun.* **2010** Oct 8, 401(1), 37–41.
5. Piret, J. *et al.* Novel Method Based on Real-Time Cell Analysis for Drug Susceptibility Testing of Herpes Simplex Virus and Human Cytomegalovirus. *J. Clin. Microbiol.* **2016** Aug, 54(8), 2120–7.
6. Cymerys, J. *et al.* Primary Cultures of Murine Neurons for Studying Herpes Simplex Virus 1 Infection and Its Inhibition by Antivirals. *Acta Virol.* **2013**, 57(3), 339–45.
7. Prasad, V. *et al.* Cell Cycle-Dependent Kinase Cdk9 Is a Postexposure Drug Target Against Human Adenoviruses. *ACS Infect. Dis.* **2017** Jun 9, 3(6), 398–405.



## Testing virucides

Virucides prevent infection from occurring by nonspecifically deactivating viruses that are present on solid surfaces (such as countertops) or in solutions. This contrasts with antiviral drugs that mitigate infection by specifically inhibiting critical viral proteins. Virucide usage is extremely common, particularly within farming, veterinary, and hospital environments. Testing the effectiveness of existing virucide formulation against a particular virus and the identification of novel virucides commonly uses a virus-induced CPE (typically in the form of a plaque assay).

E.H. Venter and colleagues evaluated the xCELLigence CPE assay as a novel means for testing virucide efficacy. They cited that, "A major problem with the testing of virucidal efficacy using current protocols is that scoring of virus-induced cytopathic effect is dependent on subjective visual interpretation using light microscopy." A commercially available chemical disinfectant/virucide was incubated with infectious bursal disease virus (IBDV) for 20 minutes. The virus was then diluted serially, and added to confluent Vero cells in E-Plates. The untreated virus caused a cytopathic effect, with the time of CPE onset dependent on the virus dilution factor (the higher the dilution, the longer it takes for killing to occur, as demonstrated in Figure 12A). However, pretreatment of IBDV with virucide significantly diminished infectivity. The 10x dilution of virus was able to induce a CPE, but 100x and higher dilutions of the virus had no effect on the Vero cells (Figure 12B).

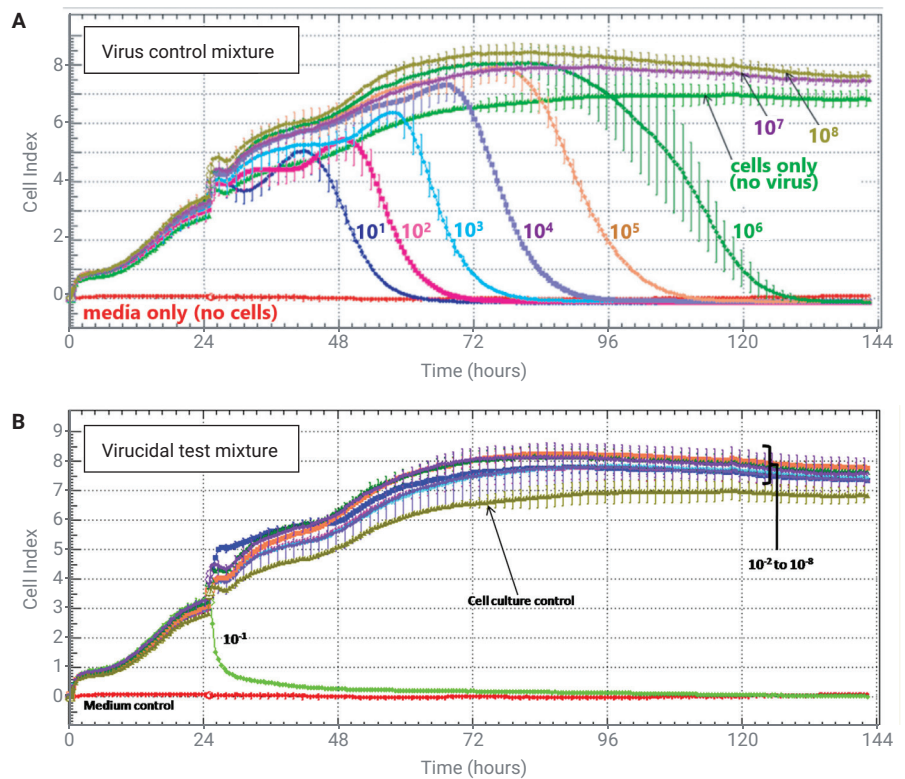


**Figure 12.** Measuring cytopathic effect of (A) virus dilutions, and (B) virus-virucide mixture dilutions on Vero cells (DVV assay) as scored using the xCELLigence system. Each curve is composed of CI values from three independent replicates. Cell index values were measured at 30-minute intervals following mixture addition. A CI value of zero indicates complete detachment of cells from the bottom of the cell culture wells. Standard deviations are indicated for each reading/curve by error bars. After exposure to virucide (B), only the most concentrated solution of virus is able to induce a cytopathic effect. Virus concentrations are denoted as fold dilutions (that is, 10<sup>1</sup> = 10x dilution, 10<sup>2</sup> = 100x dilution, and so forth).

Reprinted from the *Journal of Virological Methods*, volume 199, Ebersohn, K. et al. "An Improved Method for Determining Virucidal Efficacy of a Chemical Disinfectant Using an Electrical Impedance Assay," pages 25–28. Copyright 2014, with permission from Elsevier.

**Note:** The rapid killing observed with the 10x dilution of virucide-treated virus is likely due to a combined effect of active virions and residual virucide both acting on the target cells, suggesting that at higher concentrations the virucide is toxic to Vero cells.

In light of the above data, the authors concluded, "Although the modified [virucide] assay using the xCELLigence system yielded identical results as the traditional [virucide] assay, the system allows virucidal efficacy and cytotoxicity to be measured in a more precise and reproducible fashion."

1. Ebersohn, K.; Coetzee, P.; Venter, E. H. An Improved Method for Determining Virucidal Efficacy of a Chemical Disinfectant Using an Electrical Impedance Assay. *J. Virol. Methods*. 2014 Apr, 199, 25–8.

## Oncolytic viruses

Oncolytic virotherapy is a promising cancer therapeutic option that uses a replication-competent virus to selectively infect and kill cancer cells. While this approach can use wildtype viruses, a great deal of research is being done with viruses that are genetically engineered to achieve higher specificity or efficacy. Engineering an oncolytic adenovirus to express a secreted form of a bi-specific T cell engager to recruit cytotoxic T cells to residual cancer cells is one such example.<sup>1</sup>

With the ability to monitor cancer cell killing continuously and with high sensitivity, the xCELLigence instruments are efficient tools for quantitatively assessing the efficacy of oncolytic viruses alone or in combination with other therapeutic modalities.

In Figure 13, xCELLigence was used to monitor killing of A549 lung cancer cells by a chimeric adenovirus (Enadenotucirev, EnAd), which infects cells by binding to CD46 or desmoglein, both of which are expressed on diverse carcinomas. In a potency analysis, the cytotoxicity (killing kinetics) of EnAd at a range of concentrations was compared with wild-type adenoviruses Ad11p and Ad5. At the highest concentration (red, 500 particles per cell (PPC)), both EnAd and Ad11p caused complete cell killing (CI decreasing to zero) between 36 and 48 hours postinfection. However, at lower virus concentrations (0.8 to 20 PPC), EnAd was substantially more potent than Ad11p, displaying an earlier onset of cytotoxicity and a more rapid completion of cytolysis. When compared with EnAd and Ad11p, wildtype Ad5 was much less efficient at killing the cancer cells, requiring five days to achieve full cell killing even at the highest virus concentration. Collectively, these data highlighted the ability of xCELLigence assays to quantitatively capture differences in the potency of different oncolytic viruses.

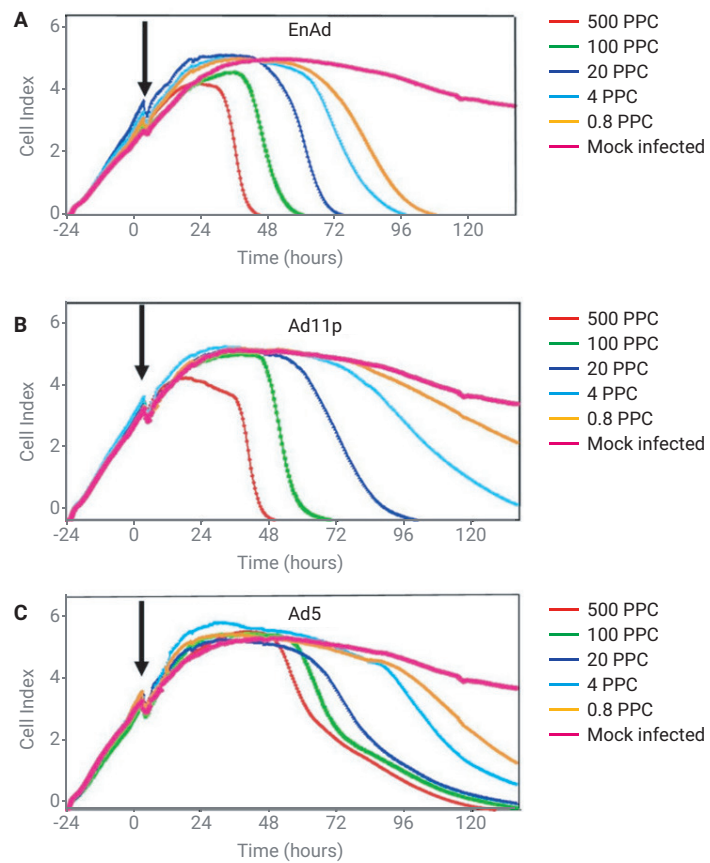


**Figure 13.** Killing of A549 lung cancer cells by different adenoviruses. Black arrows indicate the time of virus addition. Virus concentrations are listed as PPC.

Figure adapted from *Molecular Therapy Oncolytics*, volume 10(4), Dyer, A. et al. "Oncolytic Group B Adenovirus Enadenotucirev Mediates Non-Apoptotic Cell Death with Membrane Disruption and Release of Inflammatory Mediators," pages 18–30. This work is licensed under the Creative Commons Attribution 4.0 International License.

To view a copy of this license, visit <http://creativecommons.org/licenses/by/4.0/> or send a letter to Creative Commons, PO Box 1866, Mountain View, CA 94042, USA.

References—using  
xCELLigence to study  
oncolytic viruses

1. Freedman, J. D. *et al.* Oncolytic Adenovirus Expressing Bispecific Antibody Targets T-Cell Cytotoxicity in Cancer Biopsies. *EMBO Mol. Med.* **2017** Aug, 9(8), 1067–1087.
2. Fajardo, C. A. *et al.* Oncolytic Adenoviral Delivery of an EGFR-Targeting T-cell Engager Improves Antitumor Efficacy. *Cancer Res.* **2017** Apr 15, 77(8), 2052–2063.
3. Dyer, A. *et al.* Oncolytic Group B Adenovirus Enadenotucirev Mediates Non-Apoptotic Cell Death with Membrane Disruption and Release of Inflammatory Mediators. *Mol. Ther. Oncolytics* **2016** Dec 10, 4, 18–30.
4. Ellerhoff, T. P. *et al.* Novel Epi-Virotherapeutic Treatment of Pancreatic Cancer Combining the Oral Histone Deacetylase Inhibitor Resminostat with Oncolytic Measles Vaccine Virus. *Int. J. Oncol.* **2016** Nov, 49(5), 1931–1944.
5. Lacroix, J. *et al.* Oncolytic Effects of Parvovirus H-1 in Medulloblastoma are Associated With Repression of Master Regulators of Early Neurogenesis. *Int. J. Cancer.* **2014** Feb 1, 134(3), 703–16.
6. El-Andaloussi, N. *et al.* Generation of an Adenovirus-Parvovirus Chimera with Enhanced Oncolytic Potential. *J. Virol.* **2012** Oct, 86(19), 10418–31.
7. Fecker, L. F. *et al.* Efficient and Selective Tumor Cell Lysis and Induction of Apoptosis in Melanoma Cells by a Conditional Replication-Competent CD95L Adenovirus. *Exp. Dermatol.* **2010** Aug, 19(8), e56–66.

## Characterizing virus quality/fitness

When assessing the degree to which a live viral vaccine has been attenuated, comparing the cytolytic properties of two different field isolates, or probing the function of a viral gene, fitness comparisons are integral to both vaccine development and basic virology research. Although "fitness" can be defined differently within different contexts, it often refers to how efficiently a virus is able to pass through its lifecycle—spanning everything from the initial binding of cell surface receptors to genome replication, capsid assembly, and progeny viruses ultimately being released from the cell to start a new round of infection. xCELLigence-based assays are well suited for virus fitness studies because they can detect changes in the host cell throughout the continuum of a virus-induced CPE, and track these changes in real time.

Viral hemorrhagic septicemia virus (VHSV) has a negative strand RNA genome that contains a highly conserved nucleotide sequence at its 3' terminus. This was predicted to form a hairpin structure (Figure 14A). Øystein Evensen and colleagues sought to understand whether this sequence has an effect on VHSV replication and transcription in fish epithelial cells. Working with a panel of VHSV mutants, total positive strand RNA levels were quantified using qPCR two days postinfection. Figure 14B shows that, whereas the U8C and A7C-U8A mutants had no discernable impact on viral positive strand RNA levels, the A4G-G5A mutant reduced viral RNA levels significantly. xCELLigence was then used to assess the relative fitness of these different mutants (Figure 14C; virus was added to cells at the 72 hour time point). Consistent with its reduced RNA levels, the A4G-G5A mutant (green curve) required a much longer time than WT virus (black curve) to finish killing the target cells.

Interestingly, the A7C-U8A mutant (blue curve) also showed a delayed onset of CPE even though its RNA levels were equivalent to WT. Moreover, the U8C mutant (red curve) was actually more efficient than WT at killing target cells, despite having similar levels of RNA.

This example from VHSV highlighted that single time point biomarker (such as RNA) quantification can be misleading when it comes to evaluating viral fitness. It also demonstrated the utility of a functional assay that tracks the lifecycle of the virus.

Another example of xCELLigence used to quantitatively evaluate viral fitness involves bluetongue virus, which causes an economically important haemorrhagic disease in wild and domestic ruminants (cows, sheep, and goats). Bluetongue virus has a dsRNA genome that is arranged in 10 different linear segments. By nature of this genome architecture, and the fact that multiple strains of the virus can infect a cell at the same time, bluetongue virus displays substantial genetic reassortment over time. An important question is how this genome rearrangement affects the cytopathogenicity of the virus.

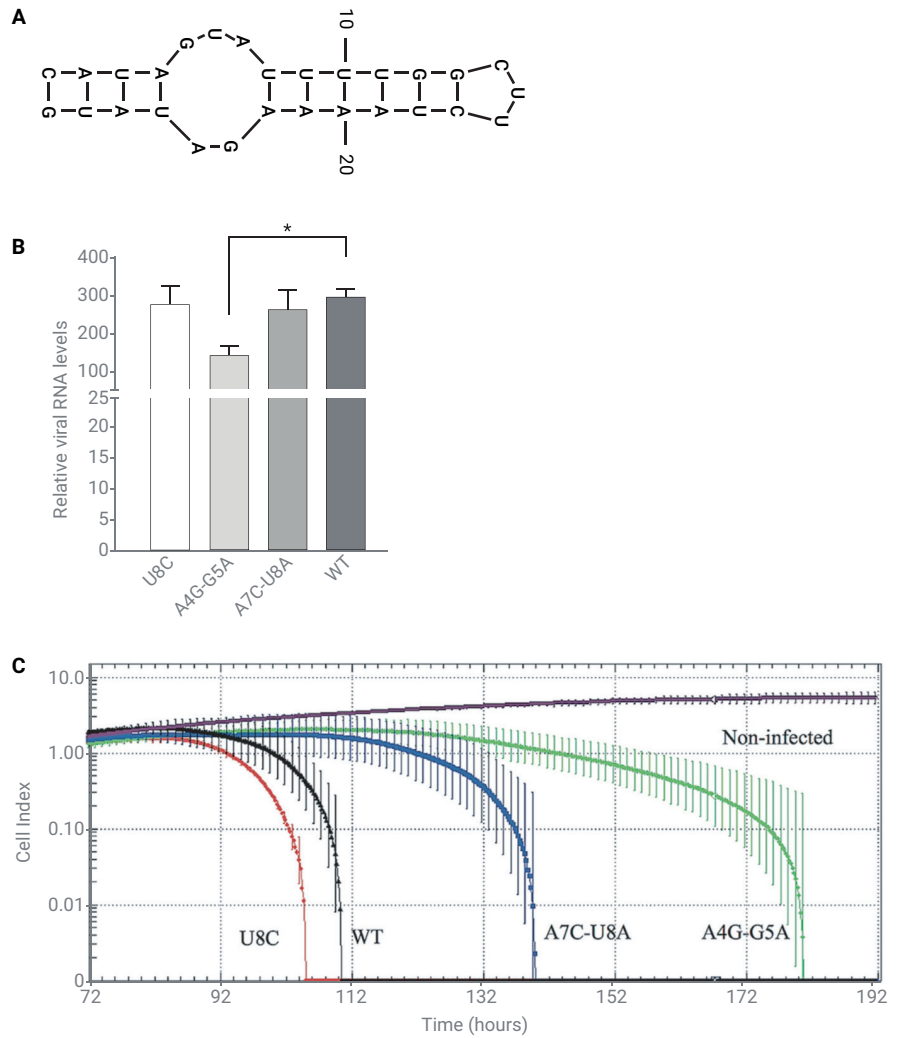


**Figure 14.** The 3' terminal sequence of the VHSV genome has an impact on both viral fitness and RNA levels. (A) Predicted secondary structure of the 3' terminus of the VHSV genome. (B) Total VHSV positive strand RNA levels two hours postinfection. (C) Quantifying the relative fitness of VHSV mutants using Agilent xCELLigence.

Figure adapted from *Virology*, volume 476, Kim, S. H. *et al.* "Specific Nucleotides at the 3'-Terminal Promoter of Viral Hemorrhagic Septicemia Virus are Important for Virulence In Vitro and In Vivo," pages 226–32. Copyright 2015, with permission from Elsevier.

Estelle Venter and colleagues investigated this by generating variants of the virus where the bulk of the genome was derived from one strain. They also included a fragment from a different strain. The team then monitored the ability of these reassortant strains to kill Vero cells in real time. As seen in Figure 15, parental strain 8 killed the target cells much more efficiently than parental strain 6. Combining strain 6 with a fragment of strain 8 did not improve its cytopathogenicity; the killing kinetics of this chimera are slower (pale blue data trace). Conversely, combining strain 8 with a fragment of strain 6 yields a virus with superior cell killing capabilities (purple data trace).

This ability to precisely track these different viral phenotypes enabled the authors to draw important conclusions about how bluetongue virus is likely to behave in the wild. Crucially, if a live attenuated strain of bluetongue virus were used to vaccinate animals, it could potentially rearrange with other strains of the virus *in vivo*, and move beyond the attenuated phenotype to achieve viremias high enough to result in *bona fide* disease.

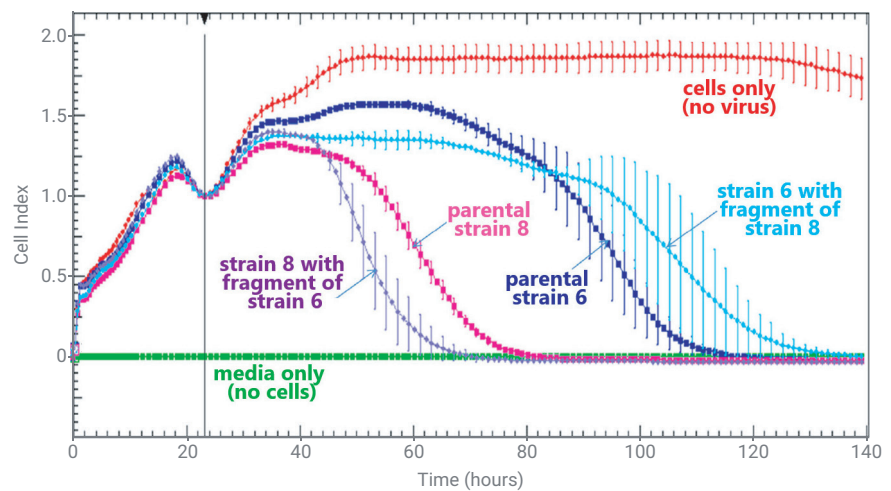


**Figure 15.** Reassortment of the bluetongue virus genome gives rise to differences in cytopathogenicity. Vero cells were grown to confluence, then infected (at 23 hours) with identical MOIs of either parental strains or genetic reassortant strains.

Figure reprinted from *Veterinary Microbiology*, volume 171 (1-2), Coetzee, P. *et al.* "Viral Replication Kinetics and *In Vitro* Cytopathogenicity of Parental and Reassortant Strains of Bluetongue Virus Serotype 1, 6 and 8," pages 53–65. Copyright 2014, with permission from Elsevier.

## References—using xCELLigence to study virus quality/fitness

1. Sung-Hyun, K. *et al.* Specific Nucleotides at the 3'-Terminal Promoter of Viral Hemorrhagic Septicemia Virus are Important for Virulence *In Vitro* and *In Vivo*. *Virology* **2015** Feb, 476, 226–32.
2. Coetzee, P. *et al.* Viral Replication Kinetics and *In Vitro* Cytopathogenicity of Parental and Reassortant Strains of Bluetongue Virus Serotype 1, 6 and 8. *Vet. Microbiol.* **2014** Jun 25, 171(1-2), 53–65.

For Research Use Only. Not for use in diagnostic procedures.

DE.5845601852

This information is subject to change without notice.

© Agilent Technologies, Inc. 2019  
Published in the USA, November 1, 2019  
5994-1086EN